J Stat Phys (2010) 141: 201–216
DOI 10.1007/s10955-010-0049-y

Mean Extinction Time in Predator-Prey Model

Matt Parker · Alex Kamenev

Received: 20 April 2010 / Accepted: 13 August 2010 / Published online: 2 September 2010

Abstract A basic predator-prey (Lotka-Volterra) system exhibits marginal stability on the deterministic level. Intrinsic demographic stochasticity destroys this stability and drives the system toward extinction of one or both species. We analytically calculate the mean extinction time of such a system and investigate its scaling with the system's parameters. This mean extinction time, measured in number of population cycles, scales as the square root of the size of the smaller population and as the minus three halves power of the size of the larger population. The analytic results are fully confirmed by Monte-Carlo simulations.

Keywords Lotka-Volterra · Extinction · Individual-based modeling

1 Introduction

One of the fundamental problems studied in population dynamics is the predator-prey model first introduced by Lotka [1] and Volterra [2]. Such a system consists of two species where one propagates itself by consuming the other. A deterministic population-based modeling of the system results in stable oscillations in the two population sizes. The system can be more accurately represented using an individual-based modeling. In this type of modeling, the populations are taken to be strictly discrete and individual birth/death events occur stochastically. This individual-based modeling inevitably forces the system to extinction by these stochastic fluctuations. Since this is considered ecologically infeasible, many authors have investigated models which stabilize or destabilize this system through the inclusion of density-dependent effects [3, 4]. Such effects change a species' per capita growth rate as the population size changes. For example, modifying the model to include an increasing fitness of the species with population density (Allee effect) may destabilize a predator-prey system [5]. More complex predator-prey systems can also create a stability. The introduction of protected prey refuges may prevent prey extinction [6]. Introducing a weakening parasitic infection in the prey species can allow for predator persistence [7]. Additional stabilization

M. Parker (✉) · A. Kamenev
School of Physics and Astronomy, University of Minnesota, Minneapolis, MN 55455, USA
e-mail: park0523@umn.edu

can arise from spatial heterogeneity in the system. These spatial variations can arise from the intrinsic stochasticity of an individual-based modeling [8] or from external enforcement [9].

It is our intent to better understand the density-independent system by calculating the mean extinction time under varying reaction conditions. This extinction time varies widely for finite systems. In fact, it is possible to construct "small" systems which persist much longer than systems which have much larger characteristic population sizes. Although all such systems are destined for extinction, additional persistence time provided under certain conditions could prove biologically important when combined with other effects such as the ones discussed previously.

A key feature of the Lotka-Volterra model is an integral of the mean-field motion which makes the mean-field trajectories neutrally stable [10]. Fluctuations are then neither amplified or damped, and thus large deviations from the mean-field results, such as extinctions, can be the result of many small step fluctuations. These small fluctuations are the result of the intrinsic demographic stochasticity of the model and result in extinction times that exhibit power law dependence on the population sizes. In contrast, in systems with stable limit cycles, extinction times are exponentially long.

The characteristic size of the populations can be defined as their value at the mean-field coexistence fixed point. The central finding of this paper is that the number of oscillations, C, for a system starting at this coexistence fixed point before the system goes extinct scales as

$$C \propto {N_S}^{3/2} \times {N_L}^{-1/2}, \tag{1}$$

where $N_L > N_S$ are the characteristic sizes of the larger and smaller populations respectively. This is a surprising result that implies, for example, that as the characteristic size of the larger population increases the system goes extinct more quickly. Further, systems that have widely differing parameters can behave virtually identically with respect to extinction time so long as the typical number of cycles, C, is the same in both systems.

This result is in agreement with previous work analyzing the scaling of this system in the long and short time limits [11]. In that work, a method of averaging stochastic fluctuations around a mean-field orbit was used to reduce the system to one dimension. The relative extinction time was calculated in very short-lived systems using a semi-classical analysis. An eigenvalue calculation was used for long-lived systems. In this paper, we extend this work by calculating a more directly measured quantity, the mean extinction time, that incorporates all Monte-Carlo trials both long and short-lived. In addition, simulations here are done using the Gillespie algorithm which is faster and more accurate than the discrete time Monte-Carlo simulations done previously.

We present here an analytic treatment of the Lotka-Volterra system using a Fokker-Planck approximation. Using an inherent separation of time scales, this two-dimensional equation can be reduced to one dimension. This equation is equivalent to diffusion over a finite interval in a specific potential. A similar averaging procedure in a Langevin formulation has recently been investigated in [12]. We then solve for the mean first passage time of this one-dimensional problem.

In Sect. 2, we review the results of a mean-field treatment of the model. Results of Monte-Carlo simulations of an individual-based model are presented in Sect. 3. An analytic approach to the calculation of the mean-extinction time is presented in Sect. 4. Finally, the results are discussed in Sect. 5.

2 Mean Field Theory

The basic predator-prey system consists of two populations. The prey reproduce at rate μ, and the predators die at rate σ. There is a third reaction in which a predator consumes one of the prey population at rate λ to reproduce. These three reactions can be summarized as

$$F \xrightarrow{\sigma} 0; \quad R \xrightarrow{\mu} 2R; \quad F + R \xrightarrow{\lambda} 2F, \tag{2}$$

where F signifies a predator ("fox") and R signifies a prey individual ("rabbit").

In a mean-field modeling, the two populations are taken to be continuous and the system's evolution is governed by deterministic differential equations. If q_1 represents the predator population and q_2 represents the prey population these equations are

$$\begin{aligned} \dot{q_1} &= -\sigma q_1 + \lambda q_1 q_2, \\ \dot{q_2} &= \mu q_2 - \lambda q_1 q_2. \end{aligned} \tag{3}$$

There are three stable states in this system. These being $(q_1, q_2) = (0, 0), (0, \infty)$, and $(\mu/\lambda,\sigma/\lambda)$. The first corresponds to the trivial case of extinction of both species. The second is an absorbing state where the predators are extinct and the prey population is growing exponentially. Finally, the third is a coexistence fixed point, where the stable populations of the predator and prey are $N_1 = \mu/\lambda$ and $N_2 = \sigma/\lambda$.

These mean-field equations of motion (3) have an integral of motion:

$$G = \lambda q_1 - \mu - \mu \ln(q_1\lambda/\mu) + \lambda q_2 - \sigma - \sigma \ln(q_2\lambda/\sigma). \tag{4}$$

The result of this constant is that the mean-field evolution of the system in predator-prey space for a given set of initial conditions is a closed orbit. In fact, the presence of this integral makes all of these closed orbits marginally stable. Fluctuations may push the system between neighboring orbits, but there is neither an opposing or restoring force to these fluctuations. The definition of G is chosen so that at the mean-field fixed point (far from extinction) $G = 0$

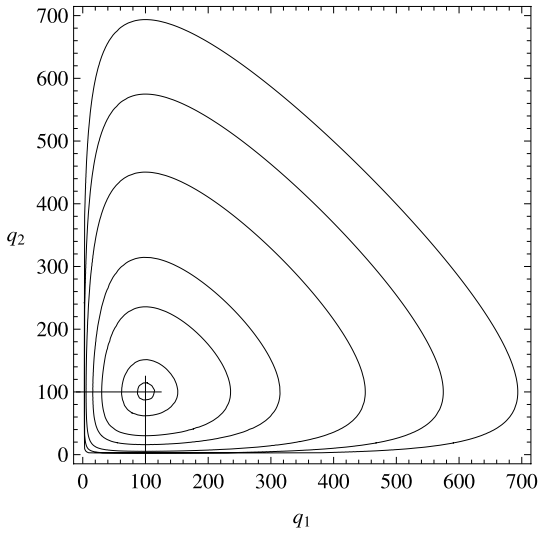

Fig. 1 Orbits of constant $G = (0.01, 0.1, 0.5, 1, 2, 3, 4)$ in units of $\sqrt{\sigma\mu}$. The evolution proceeds clockwise around the mean-field fixed point of $N_1 = N_2 = 100$

and for large cycles that closely approach the two axes, $G \to \infty$. This makes G a natural radial coordinate. Figure 1 presents orbits for various values of the integral of motion, G, for the case $N_1 = N_2 = 100$. Mean-field motion is clockwise around one of these orbits.

In the limit $G \to 0$, the mean-field cycles move along elliptical orbits with frequency $\sqrt{\sigma\mu}$. This frequency provides a natural time scale for the problem which allows a reduction of the number of parameters from the three original reaction rates to two. It is convenient to choose the parameters as

$$N = \frac{\sqrt{\mu\sigma}}{\lambda} = \sqrt{N_1 N_2}; \qquad \epsilon = \sqrt{\frac{\sigma}{\mu}} = \sqrt{\frac{N_2}{N_1}}. \tag{5}$$

Here, N represents the effective system size, while ϵ represents the asymmetry between the predator and prey populations at the mean-field fixed point. We are interested in studying the system in the limit that $N \gg 1$. For reasons explained in Sect. 4, ϵ will be restricted to values such that $N^{-1/2} < \epsilon < N^{1/2}$.

3 Stochastic Simulation

Modeling the system deterministically fails to take into account the intrinsic stochasticity associated with individual birth/death events. The inclusion of these fluctuations leads to a qualitative change in the behavior of this model. This failure of the mean-field modeling can be seen in the results from Monte Carlo simulation.

Stochastic simulations were run using the Gillespie algorithm [13] until one of the populations went extinct. In such a simulation q_1 and q_2 are taken to be strictly discrete. Births and deaths occur one at a time at a probability calculated based on the reaction rates and current populations sizes. Unless otherwise noted, the initial conditions were taken to be at the coexistence fixed point. An example of such a simulation is shown in Fig. 2. Although the clockwise-rotation that was present in the mean-field case is still observed, there is now a slow diffusion toward larger orbits. Eventually the system hits either the q_1 or q_2 axis and

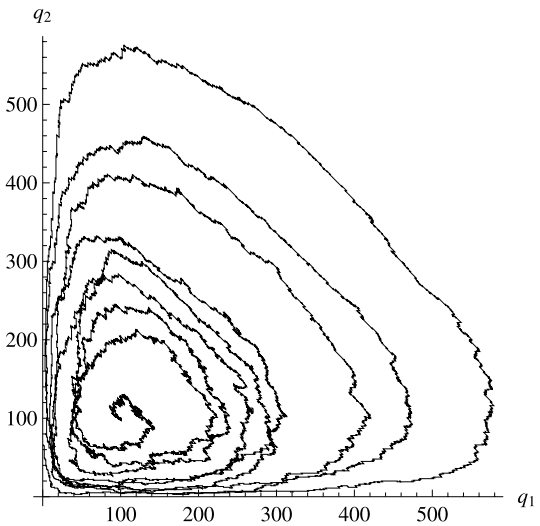

Fig. 2 Typical run of the stochastic simulation of the model (2) for $N = 100$ and $\epsilon = 1$

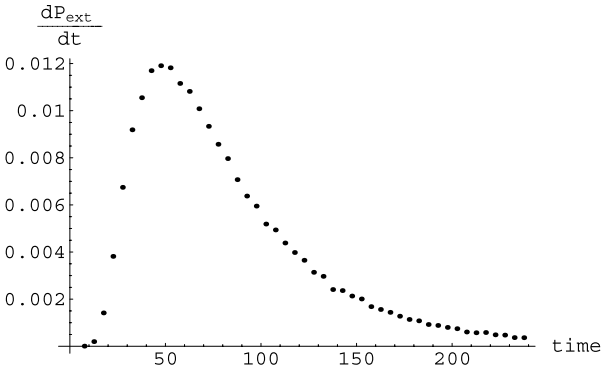

Fig. 3 Differential extinction time calculated from 10^5 simulations ($N = 100$, $\epsilon = 1$). Time is in units of $1/\sqrt{\sigma\mu}$

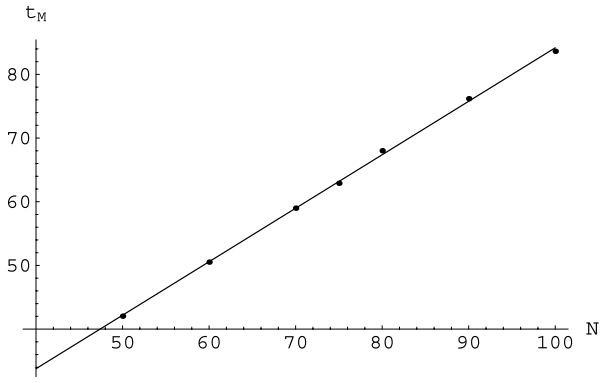

Fig. 4 Dependence of t_M on N for $\epsilon = 1$

from there rapidly moves to one of the extinct absorbing states. For a typical simulation, there are many cycles around the mean-field fixed point before an extinction event.

For a given set of initial conditions, it is possible to determine the probability of the system being extinct at a given time by repeatedly running a stochastic trial. Using these extinction times, the differential extinction probability, dP_{ext}/dt, can be plotted. Figure 3 presents the result of 100,000 trials using the conditions of the simulation presented in Fig. 2. The inevitability of extinction leads to the condition

$$\int_0^\infty \frac{dP_{ext}}{dt} dt = 1. \tag{6}$$

As could be expected, at both long and short times extinction events are unlikely.

Since such a simulation invariably ends in the extinction of one or both species, it is interesting to analyze the mean time before a given system goes extinct, t_M, given by

$$t_M = \langle t_{ext} \rangle = \int_0^\infty dt\, t \frac{dP_{ext}}{dt}. \tag{7}$$

Figure 4 shows the dependence of t_M on N. One observes a linear growth of the characteristic time t_M with increasing N at $N \gg 1$. This agrees with the results observed by Reichenbach et al. [14] for the cyclic Lotka-Volterra system. This linear dependence suggests the

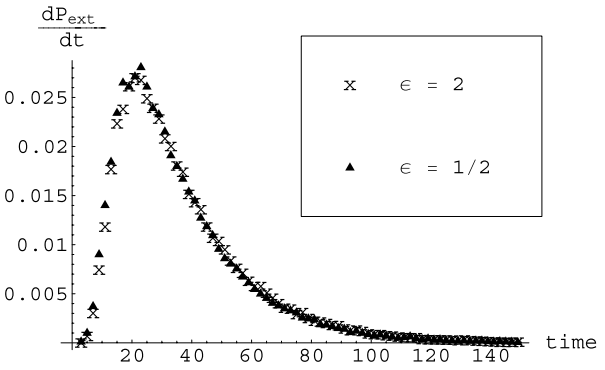

Fig. 5 Differential extinction time calculated from 10^5 simulations for $\epsilon = 2$ and $\epsilon = 1/2$; $N = 100$

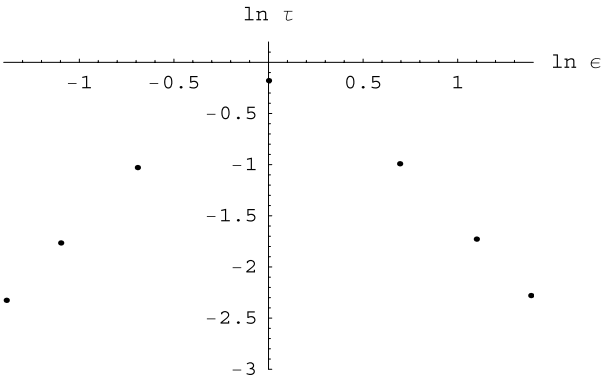

Fig. 6 Plot of $\ln \tau$ vs. $\ln \epsilon$; $N = 100$

following form for $t_M(N, \epsilon)$ in the limit $N \gg 1$:

$$t_M(N, \epsilon) = N\tau(\epsilon), \tag{8}$$

where the rescaled mean extinction time, $\tau(\epsilon)$, depends only on ϵ but not on the characteristic system size, N. The fit of Fig. 4 gives an observed value of $\tau(1) = 0.84$.

We now focus on the asymmetry parameter, ϵ. Figure 5 plots the extinction probabilities versus time for $\epsilon = 2$ and $\epsilon = 1/2$. The two models show virtually identical behavior. This similarity suggests a symmetry in τ between ϵ and $1/\epsilon$. This is confirmed by Fig. 6 which plots $\ln \tau$ vs. $\ln \epsilon$ observed from stochastic simulation, giving

$$\tau(\epsilon) = \tau(1/\epsilon). \tag{9}$$

The maximum of τ corresponds to $\epsilon = 1$. At ϵ far away from unity, a linear dependence in Fig. 6 with slope of ± 1.9 is observed. The closeness of this slope to 2 suggests that the high ϵ behavior is approximately given by $\tau(\epsilon) \propto (\max\{\epsilon, 1/\epsilon\})^{-2}$.

4 Analytic Approach

4.1 Master and Fokker-Planck Equations

The full behavior of the reaction model (2) can be analyzed by employing a probability distribution and studying its dynamics. Define $P(m,n;t)$ to be the probability of the system having m predators and n prey at time t, where m and n are both non-negative integers. This yields the following master equation

$$\partial_t P(m,n;t) = \sigma[(m+1)P(m+1,n) - mP(m,n)] + \mu[(n-1)P(m,n-1) - nP(m,n)] + \lambda[(m-1)(n+1)P(m-1,n+1) - mnP(m,n)].$$

It is possible to reformulate this master equation using a Fokker-Planck equation and further to reduce this two-dimensional Fokker-Planck equation to one dimension by using an inherent separation of time scales. The methods used were previously presented [11] and will only be highlighted here. Of particular importance is the distinction between systems with marginally stable cycles such as this one and those with stable limiting cycles or an attracting fixed point [15, 16]. In the former case, large fluctuations (such as extinctions) may proceed in a sequence of small steps. A small fluctuation leads to a mean-field like evolution along a new stable orbit until another small fluctuation shifts the orbits again. This implies that the gradients $\partial_{m,n}$ may be considered small $\sim 1/N$ which is not usually the case [17–22], and thus the master equation may be approximated as a Fokker-Planck (FP) equation which is justified by the Van-Kampen expansion over the system size N [23]. This approximation gives

$$\partial_t P = \sigma\left[\partial_{q_1} + \frac{1}{2}\partial_{q_1}^2\right] q_1 P + \mu\left[-\partial_{q_2} + \frac{1}{2}\partial_{q_2}^2\right] q_2 P + \lambda\left[\partial_{q_2} + \frac{1}{2}\partial_{q_2}^2 - \partial_{q_1} + \frac{1}{2}\partial_{q_1}^2 - \partial_{q_1}\partial_{q_2}\right] q_1 q_2 P, \tag{10}$$

where q_1 is the number of predators and q_2 is the number of prey.

It is convenient to make the following variable transformation

$$q_1 = \frac{\mu}{\lambda} e^{\sqrt{\frac{\sigma}{\mu}} Q_1}, \qquad q_2 = \frac{\sigma}{\lambda} e^{\sqrt{\frac{\mu}{\sigma}} Q_2}. \tag{11}$$

In these coordinates, predator extinction occurs at $Q_1 = -\infty$, and prey extinction occurs at $Q_2 = -\infty$. The mean-field coexistence fixed point is now at the origin. As part of the transformation, time has been transformed to be measured in the problem's natural units, and the three reaction rates (μ, σ, and λ) have been reduced to two parameters, N and ϵ. Perhaps the most important result of the transformation is that the mean-field equations of motion acquire the Hamiltonian structure, where Q_1 and Q_2 form a canonical pair

$$\begin{aligned} \dot{Q}_1 &= -1 + e^{Q_2/\epsilon} = \partial_{Q_2} G; \\ \dot{Q}_2 &= 1 - e^{\epsilon Q_1} = -\partial_{Q_1} G, \end{aligned} \tag{12}$$

with the Hamiltonian being the mean-field integral of motion, G

$$G = \frac{1}{\epsilon}(e^{\epsilon Q_1} - 1) - Q_1 + \epsilon(e^{Q_2/\epsilon} - 1) - Q_2. \tag{13}$$

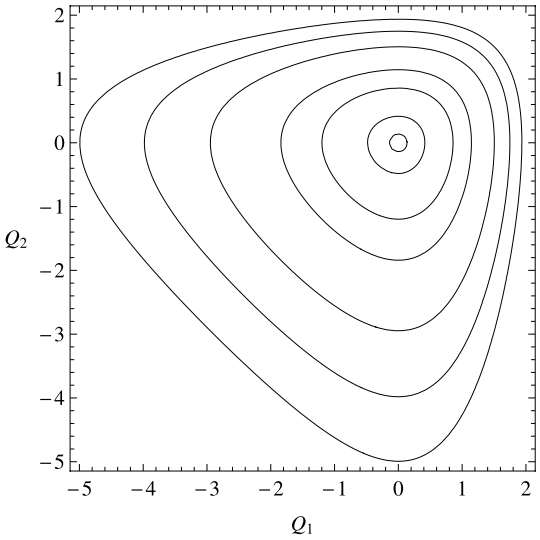

Fig. 7 Orbits of constant G in the new coordinates. Larger orbits correspond to larger values of G

As previously mentioned, G provides a natural radial coordinate. A system at the mean-field fixed point has $G = 0$ while an extinct system corresponds to $G = \infty$. Figure 7 shows mean-field orbits in the transformed coordinate system. A new probability distribution $W(Q_1, Q_2; t)$ is defined so as to include the Jacobian of the transformation

$$W(Q_1, Q_2; t) = q_1 q_2 P(q_1, q_2; t), \tag{14}$$

where q_1 and q_2 are substituted from (11). In these coordinates, the Fokker-Plank equation (10) can be represented as

$$\partial_t W = -\vec{\nabla} \cdot \left(\vec{J}^{MF} + \vec{J}^{D} \right), \tag{15}$$

where the divergence is defined as

$$\vec{\nabla} = (\partial_{Q_1}, \partial_{Q_2}). \tag{16}$$

The probability current in (15) has been broken into two parts. The first, $\vec{J}^{MF}$, is responsible for the mean-field rotation along contours of constant G, see (12). The second part of the current, $\vec{J}^{D}$, drives the radial diffusion of the system. The mean-field current is given by

$$\begin{aligned} J_1{}^{MF} &= (-1 + e^{Q_2/\epsilon}) W = (\partial_{Q_2} G) W; \\ J_2{}^{MF} &= (1 - e^{\epsilon Q_1}) W = -(\partial_{Q_1} G) W. \end{aligned} \tag{17}$$

The diffusive current is found from (10) as

$$\begin{aligned} J_1{}^{D} &= -\frac{1}{2N} \left[(e^{-\epsilon Q_1} + e^{\frac{Q_2}{\epsilon} - \epsilon Q_1}) \partial_{Q_1} W - \partial_{Q_2} W \right]; \\ J_2{}^{D} &= -\frac{1}{2N} \left[(e^{-\frac{Q_2}{\epsilon}} + e^{\epsilon Q_1 - \frac{Q_2}{\epsilon}}) \partial_{Q_2} W - \partial_{Q_1} W \right]. \end{aligned} \tag{18}$$

In particular, the diffusive current is suppressed by a factor of N relative to the mean-field current. Thus for a sufficiently large system ($N \gg 1$) the angular motion should be far faster than the radial diffusion.

4.2 Reduction to One Dimension

The mean-field constant, G, provides a natural radial coordinate. As mentioned, the corresponding angular motion is much faster. Using this time-scale separation, the two dimensional Fokker-Planck equation can be reduced to one dimension. Since Q_1 and Q_2 form a canonical pair of the mean-field system, it is possible to transform them into action-angle variables (I, α), where the action is an integral of the mean-field motion, i.e. $G = G(I)$. It is more convenient to use the parameter G instead of the canonical action, I, as the radial variable.

Since the angular motion is far faster than the radial motion, we shall assume that the probability distribution $W(G, \alpha; t)$ should rapidly equilibrate in the α direction and at long time scales should depend on G only. The probability distribution can then be represented as $W(G, \alpha) = W(G)$, and it is possible to remove the angular dependence of (15) by averaging the radial component of the current around a mean-field orbit. The transformation from (Q_1, Q_2) to (G) involves a Jacobian. This Jacobian, $T(G)$, is calculated to be the period of the mean-field orbit parameterized by G. The resulting Fokker-Planck equation is

$$T(G)\partial_t W(G) = \frac{\partial}{\partial G}\left[-\oint_G \left(\vec{J}^{MF} + \vec{J}^{D}\right)\cdot \hat{n} dl\right], \tag{19}$$

where $\hat{n}$ is a unit vector perpendicular to the line of constant G, and the integration is around a constant G contour. The mean-field current is perpendicular to $\hat{n}$ and thus makes no contribution to the integral

$$\vec{J}^{MF}\cdot\hat{n} = 0. \tag{20}$$

The integration is then only over the diffusive current, $\vec{J}^{D}$. This current is first order in both derivatives and proportional to $1/N$. Since we have assumed that there is no angular dependence to the probability distribution, the integral around the orbit may be written as

$$-\oint_G \vec{J}^{D}\cdot\hat{n} dl = \frac{1}{N} D(G)\frac{\partial W}{\partial G}, \tag{21}$$

which is in essence the definition of the effective diffusion parameter, $D(G)$. The resulting FP equation takes the form

$$T(G)\partial_t W(G,t) = \frac{\partial}{\partial G}\left[\frac{1}{N} D(G)\frac{\partial W(G,t)}{\partial G}\right], \tag{22}$$

where the two functions $D(G)$ and $T(G)$ may be evaluated for any mean-field orbit G. Both of these function depend on ϵ but are independent of the system size, N. We evaluate both of these quantities in the Appendix.

The probability distribution, $W(G, t)$, should be rescaled by the Jacobian of the transformation, $T(G)$, in order to preserve its total integral:

$$\tilde{W}(G,t) = T(G)W(G,t). \tag{23}$$

This changes (22) into

$$\partial_t \tilde{W}(G,t) = \frac{\partial}{\partial G}\left[\frac{1}{N} D(G) \frac{\partial}{\partial G}\left(\frac{\tilde{W}(G,t)}{T(G)}\right)\right]. \tag{24}$$

Since the system is incapable of moving from an extinct state to a living one, there is an absorbing boundary condition as $G \to \infty$. Since G is a radial coordinate, the current must disappear at $G = 0$. This gives boundary conditions of

$$\begin{aligned} \lim_{G\to\infty} \tilde{W}(G,t) &= 0; \\ G \frac{\partial \tilde{W}(G,t)}{\partial G}\bigg|_{G=0} &= 0, \end{aligned} \tag{25}$$

where we have employed $D(G) \sim G$ at $G \to 0$.

4.3 Reduction to the Finite Interval

Since G is formulated on an infinite interval, it is convenient to make a change to a new variable, x, such that

$$x = \int_0^G \sqrt{\frac{T(G')}{D(G')}} dG'. \tag{26}$$

Since $D(G)$ grows exponentially as $G \to \infty$ this integral is bounded. We denote this convergent value as x_0:

$$x_0 = \int_0^\infty \sqrt{\frac{T(G')}{D(G')}} dG'. \tag{27}$$

For the case $\epsilon = 1$, $x(G)$ is plotted in Fig. 8. As $G \to \infty$, x converges to $x_0 = 2.39$.

The Jacobian determinant of this transform gives a rescaled probability density of

$$\sqrt{\frac{T(x)}{D(x)}} p(x,t) = \tilde{W}(G,t), \tag{28}$$

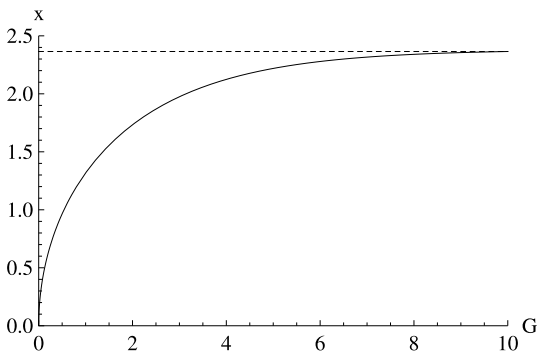

Fig. 8 $x(G)$ for $\epsilon = 1$. At $G \to \infty$ the function converges to $x_0 = 2.39$

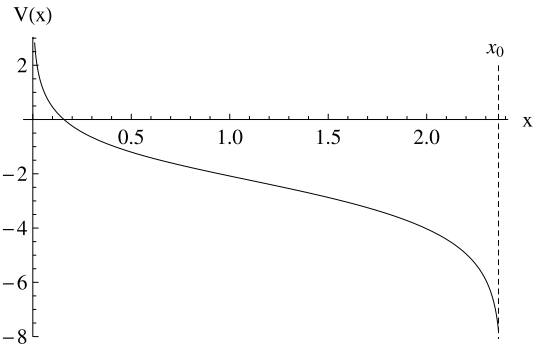

Fig. 9 Numerically calculated $V(x)$ for $\epsilon = 1$. The function diverges as $\ln(x_0 - x)$ at $x = x_0 = 2.39$

which results in a Fokker-Planck equation of

$$\partial_t p(x,t) = \frac{1}{N}\frac{\partial}{\partial x}\left[\sqrt{D(x)T(x)}\frac{\partial}{\partial x}\left(\frac{p(x,t)}{\sqrt{D(x)T(x)}}\right)\right]. \tag{29}$$

This equation is defined on the finite interval $x \in [0, x_0]$. The boundary conditions (25) take the form

$$p(x_0;t) = 0; \qquad x\frac{\partial}{\partial x}\left(\frac{p(x;t)}{x}\right)\bigg|_{x=0} = 0, \tag{30}$$

where we take into account that $\sqrt{D(x)T(x)} \sim x$ at $x \to 0$. Equation (29) no longer depends on T and D independently, but rather only on $\sqrt{TD}$ as well as the constant x_0. For brevity, we define $h(x)$ as

$$h(x) = \sqrt{T(x)D(x)}. \tag{31}$$

This changes the Fokker-Planck equation (29) into

$$\partial_t p(x,t) = \frac{1}{N}\frac{\partial}{\partial x}\left[h(x)\frac{\partial}{\partial x}\left(\frac{p(x,t)}{h(x)}\right)\right]. \tag{32}$$

This equation can be written in a more physically intuitive way:

$$\partial_t p(x,t) = \frac{1}{N}\frac{\partial}{\partial x}\left[p(x,t)\frac{\partial}{\partial x}(-\ln h(x)) + \frac{\partial}{\partial x}p(x,t)\right]. \tag{33}$$

This is simply the equation for constant diffusion in a potential, $V(x) = -\ln h(x)$. A plot of this potential for $\epsilon = 1$ is shown in Fig. 9. The two forms are equivalent, but (32) is more simple to work with and will be used for the remainder of the paper.

4.4 Mean Extinction Time

The mean extinction time, t_M, can be determined using the reverse Fokker-Planck equation. If we define the conditional probability of the system being in the state (x,t) after starting in initial conditions (y,t') as $p(x,t|y,t')$, the Fokker-Planck equation (32) becomes

$$\partial_t p(x,t|y,t') = \frac{1}{N}\partial_x\left(h(x)\partial_x\frac{p(x,t|y,t'))}{h(x)}\right). \tag{34}$$

Since the only route out of the interval $(0, x_0)$ is the absorbing boundary at x_0, if a particle is in this interval it means it has never left. The mean extinction time is then equivalent to the mean first passage time, i.e. the mean time it takes for a system to reach $x = x_0$ for the first time. The method for calculating the mean first passage time from the reverse Fokker-Planck equation is outlined by Gardiner [24]. The mean extinction time is then given by

$$t_M(x) = \langle t_{ext} \rangle = -\int_0^\infty dt t \frac{d}{dt} \left(\int_0^{x_0} dx' p(x', t|x, 0) \right), \tag{35}$$

where $x = x(G)$ is the initial position at $t = 0$. This mean extinction time must obey the following differential equation

$$\frac{1}{N} \frac{1}{h(x)} \partial_x \left(h(x) \partial_x t_M(x) \right) = -1. \tag{36}$$

Like G, x is a radial coordinate, so the current at $x = 0$ must be zero. Since there is an absorbing boundary at x_0, the boundary conditions are given by

$$\begin{aligned} t_M(x_0) &= 0; \\ \lim_{x \to 0} x \partial_x t_M(x) &= 0. \end{aligned} \tag{37}$$

The solution to (36) with these boundary conditions is given by

$$t_M(x) = N \int_x^{x_0} \frac{dy}{h(y)} \int_0^y h(z) dz. \tag{38}$$

We are first interested in the mean-extinction time for a system starting at the mean-field fixed point: $t_M = t_M(0)$.

Using the $T(G)$ and $D(G)$ behavior calculated in the Appendix and the definition of x (26), t_M can be calculated by numerical integration of (38). For the case of $\epsilon = 1$, this gives

$$t_M(\epsilon = 1) = 0.87N. \tag{39}$$

This should be compared with the mean-extinction time from stochastic simulation. Using the slope of the fit of Fig. 4, for $\epsilon = 1$ we have

$$t_M = 0.84N. \tag{40}$$

The discrepancy between these two values can be partially explained by taking into account the finite size effect. For a finite size system, it is not necessary to diffuse all the way to $G = \infty$ but only to a value of G that corresponds to a single individual remaining in one of the two populations. At this point, fluctuations will kill the system with probability close to one. This cutoff, G_{ext}, may be estimated using (4) as

$$G_{ext} = \begin{cases} \epsilon^{-1}(\ln(N/\epsilon) - 1); & \epsilon > 1, \\ \epsilon(\ln(N\epsilon) - 1); & \epsilon < 1. \end{cases} \tag{41}$$

For simulations with $N = 100$ and $\epsilon = 1$ this gives $G_{ext} = 3.62$. Integrating (26) only to G_{ext} gives $x_0 = 2.08$ (instead of $x_0 = 2.39$ for an infinite system). Similarly using this truncated x_0 as the upper integration bound in (38) gives $t_M = 0.79N$. There is only a logarithmic dependence of G_{ext} on N, so eliminating this effect from simulations is difficult.

4.5 Highly Asymmetric Case

Since $h(x)$ and x_0 are independent of N, (38) immediately shows the observed linear dependence of t_M on N. We now wish to understand the dependence of t_M on ϵ in the highly asymmetric case, that is $\epsilon \ll 1$ or $\epsilon \gg 1$. The case of $\epsilon \gg 1$ is presented here; the other case can be examined following the same line of reasoning. We first investigate the scaling of $x_0 = x_0(\epsilon)$.

In the asymmetric case, the integrand of (27) is exponentially suppressed when the high G limit of $T(G)$ becomes relevant, so $T(G)$ can be approximated as a constant. In the high ϵ limit, $D(G)$ depends only on ϵG and not on G independently. This can be understood as a consequence of the strong dependence of the stochastic noise on the population size. For $\epsilon \gg 1$, the predator population reaches far smaller populations on a given mean-field trajectory than the prey species. The stochastic noise is thus exponentially greater in the Q_1 direction than the Q_2 and can be approximated as being only in this direction. After averaging over a mean-field cycle, the result is a dependence of $D(G)$ purely on $D(\epsilon G)$. A simple rescaling of the integration variable in (27) results in the following form for x_0:

$$x_0 = \frac{\alpha}{\epsilon}, \quad \epsilon \gg 1, \tag{42}$$

where α is an ϵ and N independent constant. Using this calculation of x_0, it is possible to make a high ϵ estimation of t_M. A similar rescaling of the integration variables in (38) results in the following form of t_M in the large ϵ limit:

$$t_M = \beta \frac{N}{\epsilon^2}, \quad \epsilon \gg 1, \tag{43}$$

where like α, β is a constant that is independent of both N and ϵ. For $\epsilon \ll 1$, an analogous argument can be made, where the majority of the effects of stochastic noise are a result of Q_2 fluctuations instead of Q_1. The results are the same with $\epsilon \to \epsilon^{-1}$. This gives $x_0 = \alpha\epsilon$ and $t_M = \beta\epsilon^2 N$.

The constants α and β can be calculated from numerical integration of (38) giving

$$\begin{aligned} \alpha &= 3.1, \\ \beta &= 1.6. \end{aligned} \tag{44}$$

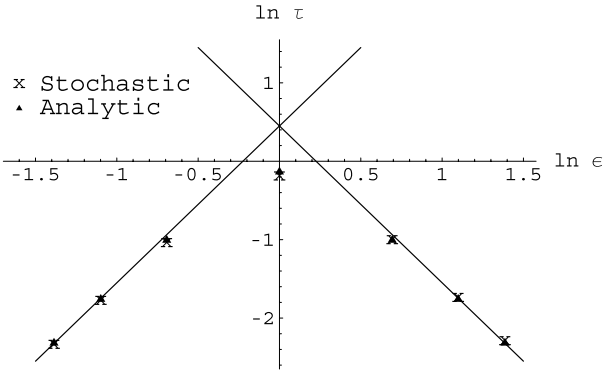

Fig. 10 Comparison of analytic and stochastic values of τ. The *lines* represented the calculated asymptotes for high and low ϵ

Figure 10 shows the results of analytic calculation for the mean extinction time compared to the results obtained from Monte Carlo simulation. The lines show the asymptotes calculated in the small and large ϵ limits. We observe good agreement between numerics and analytics. The close convergence to asymptotic calculation confirms that the mean extinction time scales as $t_M \propto N(\max\{\epsilon, 1/\epsilon\})^{-2}$. This is in agreement with what was observed in Fig. 6. Since we have relied on the separation of time scales between the angular and radial motion, it is required that there are many rotational cycles before the system goes extinct, i.e. $N > 1$. This restricts ϵ to the interval $N^{-1/2} < \epsilon < N^{1/2}$.

5 Discussion

We have investigated the mean extinction time in a Lotka-Volterra (2) system with intrinsic demographic stochasticity. Specifically, we have calculated the mean time it takes such a system to go extinct analytically and compared it with the results obtained through Monte Carlo simulations. The results showed good agreement between these values.

We consider first the asymmetric case. Recalling the definition of the parameters, (5), and employing (43) one finds

$$t_M = \beta \frac{N_S^{3/2}}{N_L^{1/2}}, \tag{45}$$

where $N_L = \max\{N_1, N_2\}$ is the size of the larger population, $N_S = \min\{N_1, N_2\}$ is the size of the smaller population, and time is measured in the natural units which is the inverse frequency of the small cycles $1/\sqrt{\sigma\mu}$. Analytic results give $\beta = 1.6$; the results of Monte-Carlo simulation are $\beta = 1.5$. This scaling relation is in agreement with results found previously for short and long-lived systems [11]. Counterintuitively, this relation predicts, for example, that the mean extinction time decreases as the larger population size increases. In fact, both populations can be increased without changing the behavior of the extinction time so long as (45) remains unchanged. To check this we performed Monte-Carlo simulations of two prey-dominated models which ought to go extinct in the same relative time. The results are presented in Fig. 11. We require that the angular motion be faster than the radial. Therefore, (45) may be trusted only if $t_M > 1$, i.e. $N_L > N_S > N_L^{1/3}$. Outside of this interval the system will typically go extinct without completing a single rotation.

We now consider the symmetric case, $N_L = N_S = N \gg 1$. We find that

$$t_M = 0.87N \to \frac{0.87}{\lambda}, \tag{46}$$

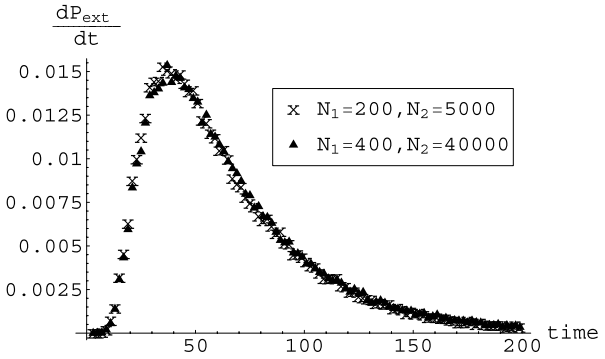

Fig. 11 Extinction probability of the two models: *crosses* $N = 1000$, $\epsilon = 5$; *triangles* $N = 4000$, $\epsilon = 10$. In both cases $t_M \approx 70$

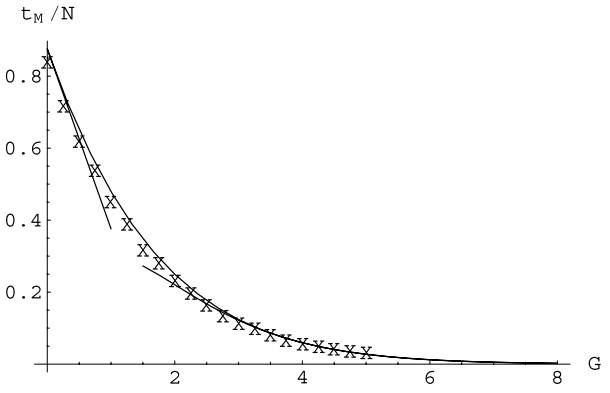

Fig. 12 Comparison of numerical integration of (38) (*full line*) and Monte Carlo values (*crosses*) of τ for varying initial values of G. The analytic calculation in the high and low G limits is also shown. ($\epsilon = 1$)

where the first result is in the relative time scale, while the second is in the absolute one. The linear scaling with the system size, N, agrees with results of Reichenbach et al. [14], obtained for a closely related cyclic model. The fact that the mean extinction time in the symmetric case is close to a half relative to the asymmetric case, (45), can be understood as follows. In the asymmetric case, the current pushing toward the extinction of the larger population is exponentially suppressed relative to the current pushing toward the extinction of the smaller and can be neglected. In the symmetric case, both of these currents are exactly the same making the extinction time twice shorter.

Further investigation can be conducted by relaxing the condition that the system begins at the mean-field fixed point. Under such a condition, the initial G will no longer be zero but begin at some positive value. Since $G = \infty$ is the condition for extinction, this means that the system will be closer to death, and the mean extinction time should be smaller. Although there is some ambiguity in the choice of initial (q_1, q_2) for non-zero G, since the angular motion is much faster than the radial, the effect of the choice should not affect the extinction time to leading order. The results of stochastic trials at varying G and the results of numerically integrating (38) are shown in Fig. 12 for $\epsilon = 1$. The small G behavior is exactly calculable and gives $t_M(G) = t_M(0) - NG/(\epsilon + 1/\epsilon)$. Of more interest is the high G behavior of $t_M(G)$. In this limit, $t_M(G) \propto Ge^{-G}$. This means that at high values of G, the system will rapidly go extinct. Alternatively, a system that is still "alive" is very likely to still be at relatively small G. Thus for a typical trial beginning near $G = 0$, the system will remain at relatively small G for the bulk of its time prior to extinction.

Acknowledgements We are indebted to M. Dykman and B. Meerson for numerous discussions. This research was supported by NSF Grant DMR-0804266 and U.S.-Israel Binational Science Foundation Grant 2008075.

Appendix: Evaluation of $D(G)$ and $T(G)$

In the limit $G \ll \min\{\epsilon, 1/\epsilon\}$, an orbit of constant G is an ellipse. Both parameters, $D(G)$ and $T(G)$, may be found exactly in this case

$$D(G) = 2\pi G(\epsilon + 1/\epsilon); \qquad T(G) = 2\pi. \tag{47}$$

Equation (22) takes the form

$$\partial_t W = \frac{\epsilon + 1/\epsilon}{N} \frac{\partial}{\partial G} \left[G \frac{\partial W}{\partial G} \right]. \tag{48}$$

Changing variables as $G = R^2$ near the mean-field fixed point gives the radial part of the two-dimensional diffusion equation with diffusion constant of $(\epsilon + 1/\epsilon)/4N$

$$\partial_t W = \frac{\epsilon + 1/\epsilon}{4N} \frac{1}{R} \frac{\partial}{\partial R} \left(R \frac{\partial W}{\partial R} \right). \tag{49}$$

The large G limit can also be estimated. The diffusive current $\vec{J}^D \cdot \hat{n}$ has two maxima corresponding to the minima in one of the two species populations. These maxima are located at $Q_2 = 0$, $Q_1 \approx -G - 1/\epsilon$ and $Q_1 = 0$, $Q_2 \approx -G - \epsilon$. Expanding the currents (18) near these two points and evaluating the integral in (21) one finds

$$D(G) = \sqrt{\frac{\pi}{2}} \left(e + \left(1 + \frac{1}{\epsilon^2} \right)^{1/2+\epsilon^2} \right) e^{\epsilon G} + \sqrt{\frac{\pi}{2}} \left(e + (1+\epsilon^2)^{1/2+1/\epsilon^2} \right) e^{G/\epsilon}. \tag{50}$$

The majority of the orbital period is spent in the third quadrant. In this quadrant, $\dot{Q}_1 \approx -1$ and Q_1 varies from $\approx -G$ to 0. This gives for the orbital period

$$T(G) = G. \tag{51}$$

Calculations using $T(G)$ and $D(G)$ were done using interpolating functions that are valid in both the high and low G limits.

References

1. Lotka, A.J.: Proc. Natl. Acad. Sci. USA **6**, 410 (1920)
2. Volterra, V.: Leçons sur la Théorie Mathématique de la Lutte Pour la Vie. Gauthier-Villars, Paris (1931)
3. Sih, A.: Theor. Popul. Biol. **31**(1), 1 (1987)
4. Neubert, M., Klepac, P., Van den Driessche, P.: Theor. Popul. Biol. **61**(3), 339 (2002)
5. Zhou, S., Liu, Y., Wang, G.: Theor. Popul. Biol. **67**(1), 23 (2005)
6. McNair, J.: Theor. Popul. Biol. **29**(1), 38 (1986)
7. Hethcote, H., Wang, W., Han, L., Ma, Z.: Theor. Popul. Biol. **66**(3), 259 (2004)
8. Wilson, W., De Roos, A., McCauley, E.: Theor. Popul. Biol. **43**(1), 91 (1993)
9. Comins, H., Blatt, D.: J. Theor. Biol. **48**(1), 75 (1974)
10. May, R.M.: Stability and Complexity in Model Ecosystems. Princeton Univ. Press, Princeton (1975)
11. Parker, M., Kamenev, A.: Phys. Rev. E **80**(2), 021129 (2009)
12. Dobrinevski, A., Frey, E.: arXiv:1001.5235v1 (2010)
13. Gillespie, D.: J. Phys. Chem. **81**(25), 2340 (1977)
14. Reichenbach, T., Mobilia, M., Frey, E.: Phys. Rev. E **74**, 051907 (2006)
15. Kamenev, A., Meerson, B.: Phys. Rev. E **77**, 061107 (2008)
16. Dykman, M.I., Schwartz, I.B., Landsman, A.S.: Phys. Rev. Lett. **101**, 078101 (2008)
17. Gaveau, B., Moreau, M., Toth, J.: Lett. Math. Phys. **37**, 285 (1996)
18. Doering, C.R., Sargsyan, K.V., Sander, L.M.: Multiscale Model. Simul. **3**, 283 (2005)
19. Dykman, M.I., Mori, E., Ross, J., Hunt, P.M.: J. Chem. Phys. **100**, 5735 (1994)
20. Elgart, V., Kamenev, A.: Phys. Rev. E **70**, 041106 (2004)
21. Assaf, M., Meerson, B.: Phys. Rev. Lett. **97**, 200602 (2006)
22. Assaf, M., Meerson, B.: Phys. Rev. E **75**, 031122 (2007)
23. van Kampen, N.G.: Stochastic Processes in Physics and Chemistry. North-Holland, Amsterdam (2001)
24. Gardiner, C.W.: Handbook of Stochastic Methods, 3rd edn. Springer, Berlin (2004)